Analytical Methods

Accepted Manuscript

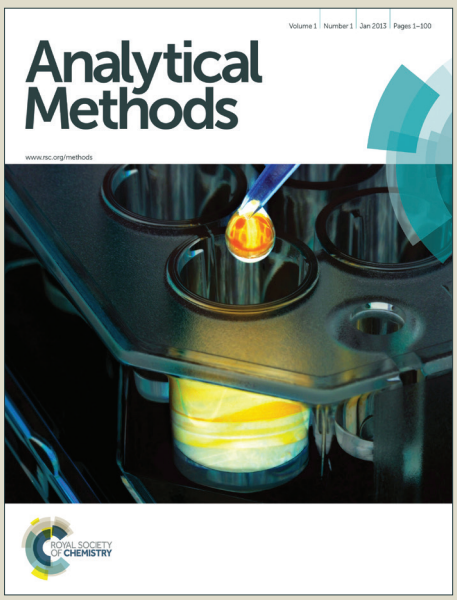

ROYAL SOCIETY OF CHEMISTRY

www.rsc.org/methods

Cite this: DOI: 10.1039/c0xx00000x

www.rsc.org/xxxxxx

Paper

Determining striatal extracellular glutamate levels in xCT mutant mice using LFPS CE-LIF

Srivani Borra,[a] Elizabeth A. McCullagh,[b] David E. Featherstone,[b,d] Phillip M. Baker,[c] Michael E. Ragozzino,[c,d] and Scott A. Shippy*[a,d]

Received (in XXX, XXX) Xth XXXXXXXXX 20XX, Accepted Xth XXXXXXXXX 20XX
DOI: 10.1039/b000000x

Glutamate analysis is useful for the study of many neurochemical processes. In-vivo sampling techniques and sample assays provide a platform for monitoring extracellular glutamate levels in the central nervous system of animal models. Low flow push pull perfusion sampling is used here to sample from the mouse striatum to understand basal extracellular glutamate levels. The 500 nL perfusate samples are pH adjusted with minimal dilution of 1.2 fold prior to derivatization for glutamate measurements. The method optimized for glutamate labelling and measurement involves the use of capillaries for addition of 100 nL solutions to samples. Quantitation of glutamate in the derivatized samples was accomplished with capillary electrophoresis-laser induced fluorescence. Glutamate and aspartate levels were monitored in C3H/HeSnJ controls and C3H/HeSnJ-Slc7a11^{sut} mutants to understand cystine-glutamate transporter (xCT) function. The study of basal glutamate levels used 4 groups: males and females of both control and mutant mice (each N=5). Using this approach, extracellular glutamate levels in mouse striatum were found to range between 2.68(±0.51) µM and 1.84(±0.40) µM. As expected, extracellular glutamate was lower in the striatum of *sut* mutant males. Control females, however, showed lower glutamate overall and no difference between genotypes. Overall, a method of LFPS collection and CE-LIF quantitation shows promise for study of glutamate in this model system.

Introduction

The composition of the extracellular fluid in biological tissues is commonly studied to better understand tissue signalling and function.[1] Common *in-vivo* sampling approaches include electrochemical measurements[2–4], microdialysis[5–7] and push-pull perfusion methods.[8–11] Low flow push pull perfusion sampling (LFPS) has been used in collecting samples from rat lateral hypothalamus[9] and rat retinas.[8,12,13] LFPS affords a number of advantages for this purpose. The dimensions of LFPS probes are relatively small compared to microdialysis and may limit tissue damage. Sample collection proceeds at the tip of the capillary-based probe that aides in site-specific collection.[11] The collection of a fluid sample allows the use of a variety of detection schemes for flexibility in the types of analytes that may be determined.[7–13] LFPS has also been used in online formats for monitoring applications.[10,14]

Glutamate is the primary excitatory neurotransmitter in the mammalian CNS. The homeostatic levels of this key molecular signal impacts glutamate-sensitive receptor function by their activation or desensitization. Besides release via synaptic vesicles, glutamate in the nervous system can be released via swelling-activated anion channels, gap junction hemi-channels, purinergic (P2X) receptors, and cystine-glutamate exchangers.[15] Cystine-glutamate transporter (xCT) is a selective amino acid transporter that exchanges extracellular cystine for intracellular glutamate. In vitro, xCT was shown to play a role in maintaining redox balance between cystine/cysteine along with its cystine uptake mechanism for glutathione synthesis during oxidative stress.[16] However xCT has also been hypothesized to play a role in maintaining extracellular glutamate levels.[15,17] Glutamate and glutathione were measured in the microdialysates of xCT$^{-/-}$ mice to understand the role of xCT in maintaining extracellular glutamate levels and oxidative stress.[18,19] The xCT system has also been studied in *D. melanogaster* where hemolymph amino acid levels were compared between controls and fly xCT mutants.[17,20] A reduction in glutamate levels was observed after loss of xCT in the *D. melanogaster* and xCT$^{-/-}$ mice model systems.[17–20] A transgenic mice model subtle gray (*sut*),[21] an xCT mutant, was used here to monitor glutamate levels in comparison to their controls.

However, there is always the question of whether measurements could be improved with less invasive techniques and for limited volume sampling regions. To better match the smaller dimension of the mouse brain, a LFPS probe developed for use in the rat eye was adopted for sampling from mouse striatum. The eye probe tip dimension is approximately 40% smaller than rat probe tip and may limit tissue damage in the mouse.[13] To improve the limit of detection of glutamate in the collected 500 nL LFPS perfusates, a method was developed to adjust the sample pH to improve fluorescence labeling. Further, this method minimizes dilutions and utilizes segments of

capillary lengths to meter out reagents. LFPS was performed on both male and female controls and mutants of xCT to determine glutamate levels and assess the role of xCT in maintaining the striatal extracellular glutamate levels.

Experimental section or Method

Chemicals and Reagents

Unless noted otherwise, chemicals were obtained from Fisher Scientific. Fluorescamine, ascorbic acid, sodium tetraborate, glutamic acid, arginine, glycine, acetone and 37% formalin solution were purchased from Sigma-Aldrich (St. Louis, MO). The composition of Krebs Ringer buffer (KRB) was 3 mM KCl, 145 mM NaCl, 1 mM $MgCl_2$, 1.2 mM $CaCl_2$, 1.61 mM $NaHPO_4$, 0.4 mM NaH_2PO_4 and 0.2 mM ascorbic acid. All solutions were prepared using 18.3 MΩ ultra filtered water (US filter, Lowell, MA). KRB and borate run buffer (pH 9) were filtered after preparation using a Millex GP 0.22 µM filter. Pentobarbital and xylazine were obtained under a controlled substance license from the UIC Pharmacy. Flexible fused silica capillaries were purchased from Polymicro technologies (Phoenix, AZ).

Low flow push-pull perfusion probe

The low flow push pull perfusion probes used to collect perfusate from the mouse striatum were of the same construction of those used to collect samples from rat retina.[13] Briefly, the fused-silica capillary dimensions of the probe include a 43-cm infusion line of 50/150 µm (id/od) tubing, a 15-cm withdrawal line of 20/90 µm (id/od) and a 4-cm probe tip of 100/170 µm (id/od) tubing. The infusion line and probe tip capillary are connected by tygon tubing. The withdrawal line was inserted through the wall of the tygon connector and threaded to the end of the probe tip.

Animals

Mice used in this study were maintained/bred at University of Illinois at Chicago. The mutant strain used for the study was C3H/HeSnJ-*Slc7a11*^{sut}, while the controls were C3H/HeSnJ. Both strains of mice were obtained from the Jackson laboratories (Bar Harbor, ME). An N of 5 for each category of controls and mutants of both male and female mice were used. All experiments were performed under a protocol reviewed and approved by the UIC Institutional Animal Care and Use Committee.

Surgical procedure

The animals were anesthetized using 50 mg/kg pentobarbital with 3 mg/kg xylazine as an analgesic. The anaesthetized mouse was positioned in the stereotaxic apparatus (Stoelting, Wooddale, IL) to install a stainless steel 29-guage guide cannula at a position +1 AP, 1.5 MP, 2 DV with respect to bregma[22]. The push-pull probe was inserted 1-mm ventrally beyond the end of the guide cannula. Supplemental doses of 10 mg/kg pentobarbital and 1.5 mg/kg xylazine were given every 40 min to maintain the anaesthesia during sampling. At the end of the experiment the animal was euthanized with an overdose of pentobarbital.

Sample collection and derivatization

Probe patency was tested before insertion with both infusion and withdrawal capillaries connected to a microsyringe filled with KRB. Continuous saline flow was monitored at the probe tip prior to insertion in to the tissue region of interest through the guide cannula. The withdrawal end was transferred to a vacuum pump via a sample-collecting tygon tubing (250 µm id) to begin withdrawal at 50 nL/min flow rate. Each sample plug volume of 500 nL was collected in 4-cm long tygon tubing.

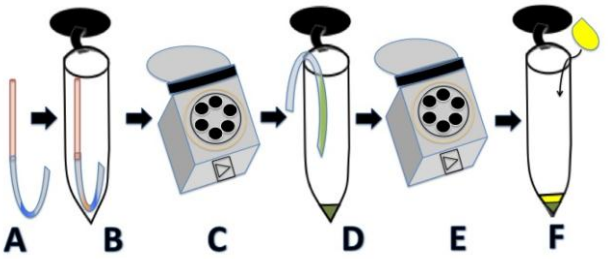

Fig.1 Schematic showing sample handling, pH adjustment and derivatization. A) Base filled capillary (Orange) connected to sample (dark blue) containing tygon tubing (light blue). B) Tygon tube along with capillary placed in centrifuge tube and C) using a bench top centrifuge to spin solution from capillary down in to tygon tube. D) The tygon tubing with 100nL base plus 500 nL sample (green) is dispensed in to a centrifuge tube using E) a bench top centrifuge. F) Addition of Fluorescamine (yellow) to pH adjusted sample in a 1:1 ratio to derivatize primary amine groups in the sample.

Perfusate sample pH was adjusted with 1:1 ratio of 20 mM borate buffer and 20 mM NaOH (hereafter referred to as base). A 100 nL volume of base was added to standards or sample as specified to adjust pH. A 2.3 mm length of 75/360 µm (id/od) capillary was filled to contain 100 nL base and connected to the sample-containing tygon tubing as shown in Figure 1A. Spinning the solution to the bottom of the injection vial using a bench top centrifuge mixed the sample with base (Fig 1B-C). Measurements of the tygon tube lengths were performed to check the total volume of the diluted sample before spinning sample from tygon into a centrifuge tube (Fig 1D-E). Reaction of primary amines with fluorescamine was performed at a 1:1 (v/v) ratio by adding 600 nL volumes of 15 mg/ml fluorescamine in acetone (Fig 1F). Reactions were for 15 min unless specified otherwise.

Capillary Electrophoresis-Laser Induced Fluorescence

The CE instrument used for these studies was built in house and the design has been previously discussed in detail.[20] In general the fluorescamine derivatized primary amines are excited at 390 nm with emission maxima centered at 475 nm.[23] The diode laser installed in our detector has a 405 nm output, which is focused on a 1-cm detection window of a 50-cm long (35 cm effective), 50/360 (id/od) fused-silica separation capillary. Fluorescence was filtered with a longpass and a broad-band filter before reaching the photon counting PMT detector. The detection system, buffers, electrodes and capillary are all positioned in a custom plexiglass box to protect the operator from high voltages. The high-voltage power supply, separation time, and the data acquisition were controlled by a custom Lab View (National Instruments, Austin, TX) program. A 30 s gravity injection at a 15 cm displacement was used to inject fluorescamine derivatized samples. The applied potential was 27 kV with a 20 mM borate run buffer.

Data analysis

Each sample or the standard was analyzed in triplicate. The

analyte peaks of the perfusate were identified by spiking with fluorescamine-labelled amino acid standards. Peak heights from individual trials were converted to concentration for analysis by a standard calibration curve. Microsoft Excel was used to plot the electropherograms, perform regressions and statistical analyses. Students' *t*-tests were performed at 95% confidence level to identify differences between groups.

Histology

Bromophenol blue was injected through the infusion end of the push-pull probe to stain the tissue at the tip of the probe. Further, the outer capillary probe tip and guide cannula were affixed with dental cement to the skull following euthanasia to help visualize push/pull perfusion tip placement. Following sample collection mouse heads with probe assembly were suspended in 10% v/v formalin solutions until histological analysis (up to 1 week). Extracted brain tissue was stored in 4% formaldehyde solutions until sectioning. Tissue was frozen and cut into 40 µm coronal sections on a cryostat. Sections were immediately mounted on slides, dried, and then, stained with cresyl violet. Placements were then verified with reference to a stereotaxic atlas.[22]

Results and Discussion

Enhancing derivatization efficiencies with small volumes

A mixture of standard arginine, glycine and glutamic acid was used to optimize derivatization conditions for 500 nL perfusate samples, which were separated using capillary electrophoresis-laser induced fluorescence (CE-LIF) to assay the amino acids. Here the reaction conditions for fluorescamine with glutamate were optimized. Parameters like buffer salt, pH, organic cosolvent and fluorescamine concentration influence the fluorophor formation and can potentially deactivate the fluorescence derivatives after formation.[24] Also, fluorescamine hydrolysis product formation competes with fluorophor formation in aqueous media by their deactivation.[24] For these reasons an optimization of fluorescamine reaction was needed for glutamate measurements in LFPS perfusates of xCT subjects. The xCT system has earlier been studied in *D. melanogaster* where hemolymph glutamate levels were determined to be 38% lower in genderblind *(gb)* mutants, which have reduced expression of a fly xCT homolog.[17,20] Since *sut* mutants carry a mutation in the mouse xCT gene (*Slc7a11*), *sut* mice might also be expected to display a similar decrease in glutamate concentration. Such a decrease may require a method that provides low limit of detection for glutamate measurements. The assay used KRB as perfusion solution to mimic the CSF composition and also to dissolve amino acid standards. The major buffer composition of the cerebrospinal fluid is a carbonate system and has a slightly basic pH up to 7.35.[25] The fluorescence tagging reaction with amino acids by fluorescamine requires pH of 8.5-9.5.[24]

To improve analyte derivatization, perfusate samples required a pH modification. However, extensive sample dilution should be avoided as xCT subjects may have less glutamate. In these studies a 100 nL volume of base was added to 500 nL samples prior to derivatization in order to improve labelling and the limit of detection. This provided a low dilution of 1.2 fold before addition of derivatization reagent. Capillaries of defined length were used to meter 100 nL volumes. By using a defined length capillary of a known inner diameter it is possible to collect and dispense a precise volume in a range of volumes down to 10's of nL. The collected sample along with the base was spun down in to the injection vial using a bench top centrifuge to enhance mixing of these nL volumes. The approach of using these capillaries towards manipulating pH of nL volumes is shown in this work by varying pH by addition of different buffer compositions and, the efficiency of derivatization.

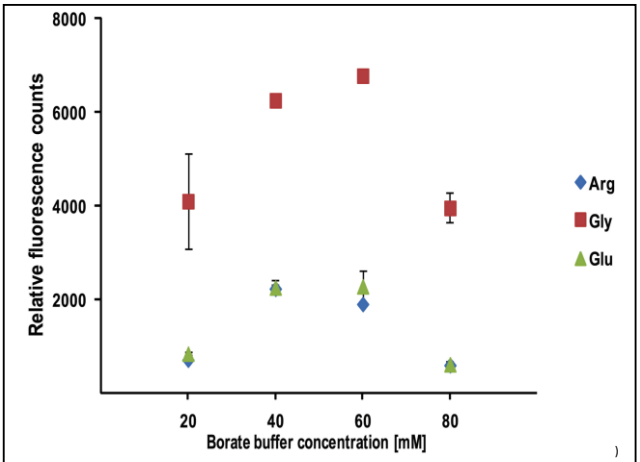

Fig.2 Optimization of pH conditions for efficient derivatization of arginine, glycine and glutamic acid by adding 100 nL of 20, 40, 60 and 80 mM borate buffer prior to derivatization. All separations were performed in 20 mM borate buffer with a 30 sec injection on a 50 cm 50/360 µm (id/od) capillary with an electric field of 540 V cm^{-1}.

Various concentrations of borate buffer were used to LFPS perfusate for efficient amino acid labelling. Sample pH was adjusted with 20, 40, 60 and 80 mM concentrations of borate buffer (Figure 2). Measurements of pH performed on 20, 40, 60 and 80 mM borate buffer showed an increase in pH from 20 to 80 mM borate buffer. An increase in the labelled amino acid signal was observed in moving from 20 to 60 mM borate buffer additions suggesting the influence of pH on fluorophor formation. Further addition of 80 mM led to a decrease in signal for all three amino acids. The decrease in reaction efficiency with the higher 80 mM borate buffer could be the result of any of a variety of borate buffer species that form at higher concentrations. The increasing buffer capacity seems to affect the derivatization beyond the change expected with an increase in sample pH. The lower reaction efficiency may alternatively be due to higher buffer ionic strength.

To explore if increasing borate buffer composition and not pH itself was limiting reaction efficiency, NaOH modified borate buffer compositions were used. Concentrated NaOH was added to 20 and 40 mM borate buffers to increase their pH beyond buffer pH. Relative fluorescence from these NaOH modified buffers is shown in Figure 3. Measured pH for these NaOH modified buffers were in decreasing order from 20 mM borate buffer: 20 mM NaOH> 40 mM borate buffer: 10 mM NaOH > 40 mM borate buffer. The A 1:1 ratio of 20 mM borate buffer: 20 mM NaOH showed maximal fluorescence among the three compositions (Figure 3) suggesting that increasing pH increases fluorescence labelling, while the same is not true with increasing pH using buffer ionic strength (Figure 2). The increasing buffer

ionic strength from 80 mM borate buffer possibly led to a decrease in reaction efficiency (Figure 2). The lower solution ionic strengths likely avoid higher concentration borate solution species while stabilizing the pH around 9.

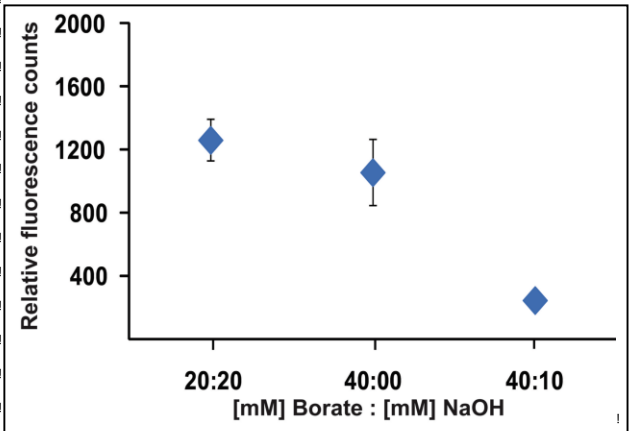

Fig.3 Optimization of pH conditions for efficient derivatization of glutamic acid by adding 100 nL of borate and NaOH mixture. 1:1 ratios of (1)20 mM borate: 20 mM NaOH, (2)40 mM borate, (3)40 mM borate: 10 mM NaOH prior to fluorescamine addition. All separations were performed in 20 mM borate buffer with a 30 sec injection on a 50 cm 50/360 µm (id/od) capillary with an electric field of 540 V cm^{-1}.

The pH for 20 mM borate buffer: 20 mM NaOH and 80 mM borate buffer were observed to be 9.35 and 9.26 respectively. Though the pH for these two were similar, the reaction efficiency was higher for 20 mM borate buffer: 20 mM NaOH than 80mM borate buffer when compared to 40 mM borate buffer. Addition of NaOH leads to more buffer capacity toward acid as evidenced by the higher pH and may neutralize the acid produced during fluorescamine reaction. Overall, a NaOH modified borate buffer shows increased labelling efficiency. A study between sodium phosphate and sodium borate buffers, showed that the hydrolysis product formation proceeded at less than half the rate in sodium phosphate compared to sodium borate buffer.[26] The decrease in fluorescence with 80 mM borate buffer observed here may also be due to the enhanced hydrolysis product formation in borate buffer. For further study of reaction kinetics and animal samples, the 1:1 ratio of 20 mM borate buffer: 20 mM NaOH was used to increase pH of the perfusate.

Derivatization kinetics of 500 nL sample volumes

Time dependent experiments were done to monitor the derivatization kinetics of the expected low micromolar concentration 500 nL LFPS samples. Reaction fluorescence was assessed at 5, 10, 15, 30, 45 and 60 min (Figure 4). The rate of the reaction with 500 nL sample volumes at 5 µM concentrations of standard mixture showed maximal average levels at 15 min and stable levels to 45 min after addition of fluorescamine. Initial reaction is fastest with primary amines but a decrease in signal was observed beyond 45 min. Previously, the reaction of fluorescamine with primary amines was reported to be in msec.[27] However, different amino acids react at different rates with fluorescamine. Acid side chain amino acids like glutamate and aspartate are reported to react slower compared to glutamine and aspargine.[28] Here arginine was observed to react faster than glycine and glutamate. The rate of reaction also depends on the cosolvent with half times ranging in fractions of an hour rather than seconds for alcoholic solvents as they form irreversible addition products.[26] For our experiments acetone was used as a cosolvent to dissolve fluorescamine at a 54 mM concentration. Fluorescamine hydrolysis products are believed to quench fluorescence signal at high concentrations and that effect may also increase with higher pH.[24,26] When using acetone as a cosolvent, the rate of hydrolysis was reported to increase from pH 9 to10.[26] The slower reaction rate and subsequent signal loss may be due to the effects of hydrolysis products and the use of acetone as cosolvent. Based on the results, 15 min reaction time was used for the optimized derivatization.

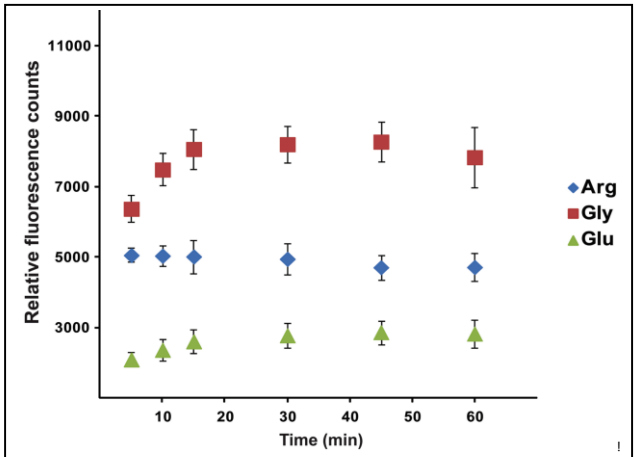

Fig. 4 Optimization of derivatization time for arginine, glycine and glutamic acid at 5, 10, 15, 30, 45 and 60 min. All separations were performed in 20 mM borate buffer with a 30 sec injection on a 50 cm 50/360 µm (id/od) capillary with an electric field of 540 V cm^{-1}.

Extracellular glutamate and aspartate concentration in mouse striatum

For the first time, LFPS was demonstrated in a mouse model system. These studies were performed with C3H/HeSnJ controls and the xCT knocked-out C3H/HeSnJ-*Slc7a11*^{sut} mutants. To better match the smaller size of the model system, the probe utilized was about 40% smaller than that developed for collecting extracellular fluid from the vitreoretinal interface of the rat.[11] Sample volumes of 500 nL were obtained using push-pull perfusion where sampling likely proceeds at the tip of the 170 µm capillary probe tip. After applying the optimized conditions for pH adjustment and derivatization time, the fluorescamine tagged samples were separated using CE-LIF. A typical electropherogram of mouse striatum perfusate is shown in Figure 5. From the electropherogram three relatively distinct regions are seen. The first two min of separation include arginine and likely other di and polyamine compounds. A less-resolved neutral amino acid region was seen between two to three min; both the amino acid glycine and fluorescamine hydrolysis products were found in that region. While fluorescamine is a fluorogenic reagent, hydrolysis products were seen which may be due to its high (~54 mM) levels used in the reaction. A third region between three to four min shows the peaks for glutamate and aspartate that are well resolved from each other (Figure 5). A S/N of 15.31 was obtained for a 0.5 µM glutamate standard and LOD (S/N=3) of 0.19 µM and an LOQ of 0.65 µM was obtained from

the optimized method. These figures of merit suggest the method is appropriate for the assay of glutamate based upon expected

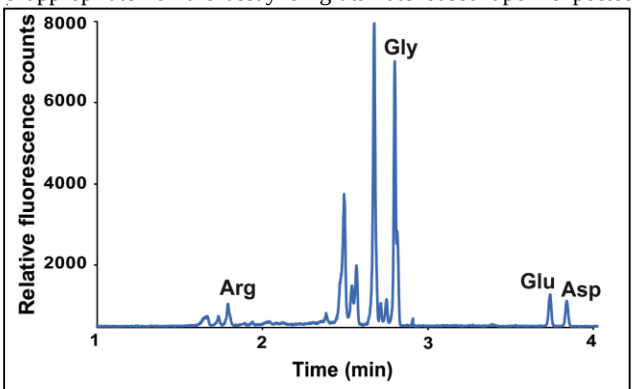

Fig. 5 Raw electropherogram of 500nL of mice cerebrospinal fluid collected from striatum using LFPS, and fluorescently tagged with fluorescamine addition after adding 100nL base. Separation conditions: 50/360 µm (id/od) fused-silica capillary, 35/50 cm effective length / total length, LIF detection with 408 nm TCEBL, 540 V cm^{-1} field strength, 15 cm/ 30 s gravity injection, run buffer: 20 mM Borate.)

sample levels of glutamate. Both glutamate and aspartate were identified and quantitated in the treated perfusate samples. Aspartic acid levels were measured as a negative control for changes in glutamate, since we have no reason to believe that aspartic acid levels would differ between *sut* mutants and controls.

The average concentration of perfusate glutamate collected from probes placed in the striatum of control mice was found to be 2.17 (±0.68) µM (N=20). The aspartic acid levels were observed to be 5.60 (±3.84) µM (N=20). The glutamate value observed here falls in between 1 to 5 µM, a range that was reported for the extracellular glutamate levels in rat striatum using microdialysis.[15] Our glutamate data compare well to the extracellular glutamate levels found in mice striatum using microdialysis sampling in CD1 strain and C57BL/6J[29,30] and an enzyme-based microelectrode array approach.[31] To our knowledge, LFPS has not yet been used to sample from mouse striatum. To demonstrate the applicability of LFPS for determining mouse neurochemistry, both control and *sut* mutants were compared for glutamate and aspartate. The summary of glutamate and aspartic levels for 5 male controls, 5 female controls, 5 male mutants, and 5 female mutants, are tabulated in Table 1a and 1b. The observed p-values from *t*-test comparison of mean concentrations are placed between compared concentrations.

Previous work in *D. melanogaster* fly model has shown 38% lower glutamate levels in fly xCT (*genderblind)* mutants compared to their controls.[20] Microdialysis experiments performed with an alternative mutant, xCT $^{-/-}$ mice, showed a 70% decrease in striatal glutamate levels.[18] Based upon this earlier work, a decrease in basal glutamate was hypothesized. A means comparison *t*-test showed a significant difference in the basal glutamate level between control and *sut* male mice (p=0.0464). However, there was no significant difference found between control and *sut* females (p=0.1688). The results from males appear consistent with previous studies showing that loss of xCT leads to loss of extracellular glutamate. Of the four model groups compared in this study, the strongest difference was found

Table 1a Average extracellular glutamate concentration (µM±standard deviation) in mice striatum of control males, control females, and xCT mutant males and females (n=5).

Control/Mutant	Male ♂		Female ♀
Control	2.68(±0.51)	*0.0121*[c]	1.84(±0.40)
	0.0464[a]		*0.1688*[b]
Mutant	1.92(±0.71)	*0.2552*[d]	2.25(±0.81)

Table 1b Average extracellular aspartate concentration (µM±standard deviation) in mice striatum of control males, control females, and xCT mutant males and females (n=5).

Control/Mutant	Male ♂		Female ♀
Control	7.27 (±3.94)	*0.0673*[c]	3.82(±2.02)
	0.3154[a]		*0.2728*[b]
Mutant	5.93(±4.50)	*0.4226*[d]	5.34(±4.76)

t-Test comparison -Sample Assuming equal variances P<0.05 between [a]control and subtle gray mutant males, [b]control and subtle gray mutant females,[c]male and female controls,[d]male and female subtle gray mutants

in basal glutamate levels of male and female controls with a p-value of 0.0121. This effect between the control male and female subjects is unusual and points to possibility of significant physiological differences based upon sex. The reason for the possible sex difference isn't clear. Notably there are also some sex-specific behavioral differences seen between control and *sut* mice (McCullagh *et al.* in prep). The fact that there were no differences found among any groups with respect to aspartate is strongly supportive of the relative accuracy of the method.

Histological analysis

To verify the sampling region and study the extent of tissue damage employing LFPS, histological analysis of the tissue was performed after sample collection. The brain slice image shown in Figure 6a is representative data from initial experiments. In the initial histological studies LFPS probes were immediately removed at the end of the sample collection, the brain tissue extracted and then fixed in 4 % formaldehyde until histological analysis. No microscopic evidence of guide or probe tracks were observed for these acute studies, after sample collection. The 170 µm (od) probe dimension of the outer infusion capillary employed for sample collection, along with the low flow rates of (10-50 nL/min) of LFPS could have minimized the tissue damage. Here LFPS was used for the first time to sample from mouse striatum. The first LFPS studies by our group were performed in striatum and lateral hypothalamus of rat, using a 27-guage, stainless steel outer cannula.[9,11] The 40% reduction in probe size and the all fused-silica capillary construction allowed the use of a 29-gauge guide tubing. Previously used LFPS employed in rat striatum showed tissue damage mostly due to the

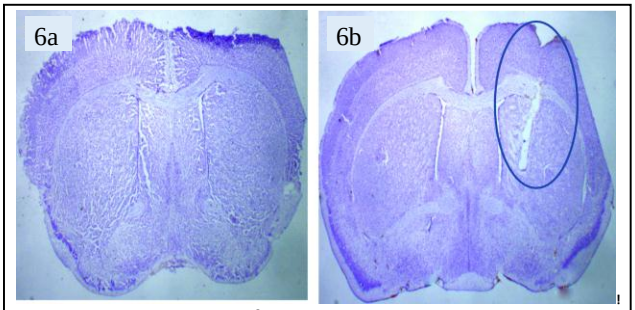

Fig. 6 Coronal section of mouse brain striatum showing LFPS probe track. 6(a) shows no microscopic evidence of LFPS probe track when probe was removed immediately after sample collection. 6(b) shows microscopic evidence of LFPS probe when the probe was left intact with the tissue until sectioning.

probe track.[11] The use of miniaturized version of LFPS here showed no probe track in histological analysis, suggesting a decrease in tissue damage compared to our previous work. A recent study of glutamate in xCT$^{-/-}$ mice employed a 240 µm (od) microdialysis probe and a larger guide cannula for sampling from mouse striatum.[18] The 29% smaller probe used in this work also provides sample collection at the capillary tip of the probe compared to the 1-mm long dialysis membrane. Given the inability of standard histological techniques to visualize even the guide cannula, electron microscopy would be required to determine the extent of tissue damage by our sampling method.

In order to create enough tissue damage to visualize and verify probe tip after glutamate measurements, guide cannula and inserted probe tip were affixed into place with dental cement following sampling. Once secured, the probe tubing extending from the subject head was cut to be even with the top of the subject head after sample collection and prior to tissue fixation. The representative histology from this tissue preparation is shown in Figure 6b. The prolonged tissue exposures to the guide cannula with LFPS probe following sample collection clearly aided in verification of probe placement. The need for enhancing tissue damage after sample collection to verify probe placement, emphasizes the minimal tissue damage advantage provided by 170 µm (od) LFPS probe. This is a distinct advantage among *in-vivo* sampling techniques and helps in supporting the physiological relevance for collecting samples from tissue regions that play an important role in behavioral and cognitive sciences. A LFPS probe smaller than 170 µm (od) probe dimension of the outer infusion capillary, can be explored in future studies to enhance the advantages of LFPS which consistently proves as a minimal invasive *in-vivo* sampling technique.

Conclusions and future directions

LFPS has been used in a mouse model for the first time. These studies of glutamate levels appear to show a relationship to the loss of xCT in *sut* male mice only, suggesting other factors contribute significantly to glutamate homeostasis. Future work may include study of sulfhydryl containing analytes in extracellular fluid. Considering the relatively small probe dimensions and extent of observed tissue damage, LFPS would likely be useful for sampling from still smaller brain regions or other tissues relevant to cognitive sciences. Also, the use of defined capillaries to meter out reagents seems promising for minimizing sample dilution while performing sample preparation with nL sample volumes.

Notes

[a] *Department of Chemistry, University of Illinois at Chicago, 845 West Taylor Street, 4323 SES, MC 111, Chicago IL 60607, USA. Tel: 31 2413 5082; E-mail: sborra3@uic.edu*

[b] *Department of Biological Sciences, University of Illinois at Chicago 840 West Taylor Street, SEL 4311, M/C 067, Chicago, IL 60607, USA.Fax: 31 2996 2805; Tel: 31 2413 2516; E-mail: def@uic.edu*

[*,a] *Department of Chemistry, University of Illinois at Chicago, 845 West Taylor Street, 5417 SES, MC 111, Chicago IL 60607, USA. Fax: (312) 996-0431; Tel: 31 2355 2426; E-mail: sshippy@uic.edu*

[c] *Department of Psychology, University of Illinois at Chicago 1007 West Harrison Street, Chicago, IL 60607, USA.*

[d] *Laboratory of Integrative Neuroscience, University of Illinois at Chicago 840 West Taylor Street, SEL 4311, M/C 067, Chicago, IL 60607, USA.*

References

1. M. Perry, Q. Li, and R. T. Kennedy, 2010, **653**, 1–22.
2. E. R. Hascup, K. N. Hascup, M. Stephens, F. Pomerleau, P. Huettl, A. Gratton, and G. a Gerhardt, *J. Neurochem.*, 2010, **115**, 1608–20.
3. M. V Avshalumov, B. T. Chen, S. P. Marshall, D. M. Peña, and M. E. Rice, *J. Neurosci.*, 2003, **23**, 2744–50.
4. N. Nakamura, K. Negishi, A. Hirano, and M. Sugawara, *Anal. Bioanal. Chem.*, 2005, **383**, 660–7.
5. D. a Baker, H. Shen, and P. W. Kalivas, *Amino Acids*, 2002, **23**, 161–2.
6. D. a Baker, Z.-X. Xi, H. Shen, C. J. Swanson, and P. W. Kalivas, *J. Neurosci.*, 2002, **22**, 9134–41.
7. M. F. Presti, C. J. Watson, R. T. Kennedy, M. Yang, and M. H. Lewis, *Pharmacol. Biochem. Behav.*, 2004, **77**, 501–7.
8. K. Thongkhao-On, S. Kottegoda, J. S. Pulido, and S. a Shippy, *Electrophoresis*, 2004, **25**, 2978–84.
9. K. Thongkhao-on, D. Wirtshafter, and S. a Shippy, *Pharmacol. Biochem. Behav.*, 2008, **89**, 591–7.
10. E. E. Patterson, J. S. Pritchett, and S. a Shippy, *Analyst*, 2009, **134**, 401–6.
11. S. Kottegoda, I. Shaik, and S. a Shippy, *J. Neurosci. Methods*, 2002, **121**, 93–101.
12. S. Kottegoda, J. S. Pulido, K. Thongkhao-on, and S. a Shippy, *Mol. Vis.*, 2007, **13**, 2073–82.
13. J. S. Pritchett, J. S. Pulido, and S. a Shippy, *Anal. Chem.*, 2008, **80**, 5342–9.
14. R. T. Kennedy, J. E. Thompson, and T. W. Vickroy, *J. Neurosci. Methods*, 2002, **114**, 39–49.
15. D. E. Featherstone and S. a Shippy, *Neuroscientist*, 2008, **14**, 171–81.
16. J. Y. Kim, Y. Kanai, a Chairoungdua, S. H. Cha, H. Matsuo, D. K. Kim, J. Inatomi, H. Sawa, Y. Ida, and H. Endou, *Biochim. Biophys. Acta*, 2001, **1512**, 335–44.
17. H. Augustin, Y. Grosjean, K. Chen, Q. Sheng, and D. E. Featherstone, *J. Neurosci.*, 2007, **27**, 111–23.
18. A. Massie, A. Schallier, S. W. Kim, R. Fernando, S. Kobayashi, H. Beck, D. De Bundel, K. Vermoesen, S. Bannai, I. Smolders, M. Conrad, N. Plesnila, H. Sato, and Y. Michotte, *FASEB J.*, 2011, **25**, 1359–69.
19. D. De Bundel, A. Schallier, E. Loyens, R. Fernando, H. Miyashita, J. Van Liefferinge, K. Vermoesen, S. Bannai, H. Sato, Y. Michotte, I. Smolders, and A. Massie, *J. Neurosci.*, 2011, **31**, 5792–803.
20. S. C. Piyankarage, H. Augustin, Y. Grosjean, D. E. Featherstone, and S. a Shippy, *Anal. Chem.*, 2008, **80**, 1201–7.
21. S. Chintala, W. Li, M. L. Lamoreux, S. Ito, K. Wakamatsu, E. V Sviderskaya, D. C. Bennett, Y.-M. Park, W. a Gahl, M. Huizing, R. a

Spritz, S. Ben, E. K. Novak, J. Tan, and R. T. Swank, *Proc. Natl. Acad. Sci. U. S. A.*, 2005, **102**, 10964–9.
22. K. B. J. Franklin and G. Paxinos, *The Mouse Brain in Stereotaxic Coordinates*, Academic Press, Amsterdam, 3rd edn., 2007.
23. S. Udenfriend, S. Stein, P. Böhlen, W. Dairman, W. Leimgruber, and M. Weigele, *Science*, 1972, **178**, 871–2.
24. S. De Bernardo, M. Weigele, V. Toome, K. Manhart, W. Leimgruber, P. Böhlen, S. Stein, and S. Udenfriend, *Arch. Biochem. Biophys.*, 1974, **163**, 390–399.
25. B. K. Siesjo, 1972, **1**, 360–374.
26. S. Stein, P. Böhlen, and S. Udenfriend, *Arch. Biochem. Biophys.*, 1974, **163**, 400–403.
27. S. Udenfriend, S. Stein, P. Böhlen, W. Dairman, W. Leimgruber, and M. Weigele, *Science*, 1972, **178**, 871–2.
28. D. Smith and F. Chen, 1978, **189**, 241–250.
29. D. Lang, C. Kiewert, A. Mdzinarishvili, T. M. Schwarzkopf, R. Sumbria, J. Hartmann, and J. Klein, *Brain Res.*, 2011, **1425**, 155–63.
30. S. S. Shakil, H. K. Holmer, C. Moore, A. T. Abernathy, M. W. Jakowec, G. M. Petzinger, and C. K. Meshul, *Synapse*, 2005, **58**, 200–7.
31. K. N. Hascup, E. R. Hascup, F. Pomerleau, P. Huettl, and G. A. Gerhardt, 2008, **324**, 725–731.

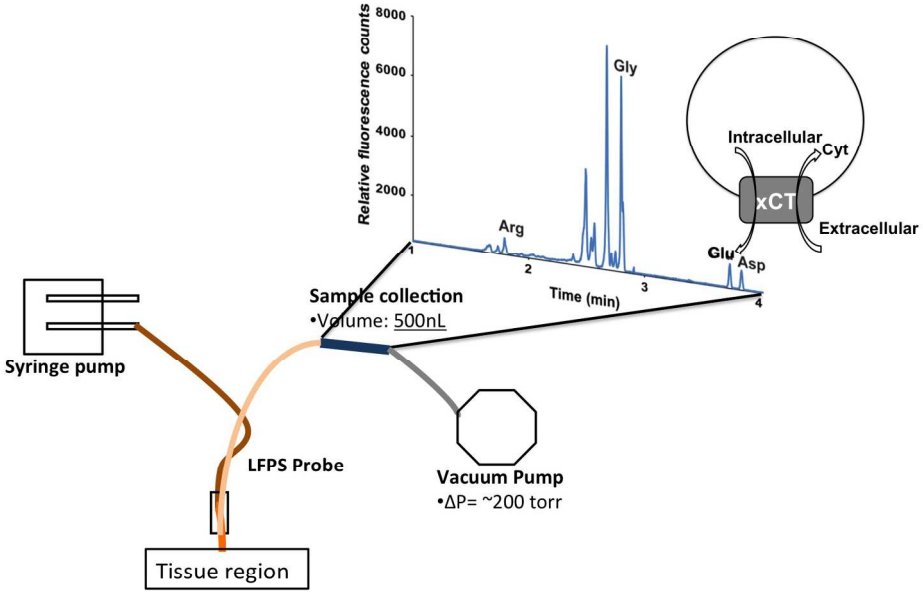

705x529mm (72 x 72 DPI)